International Journal of Biological Macromolecules 285 (2025) 138366

Contents lists available at ScienceDirect

International Journal of Biological Macromolecules

journal homepage: www.elsevier.com/locate/ijbiomac

# PRRX1/miR-143-3p signaling regulates homeostasis of antler reserve mesenchymal cells

Pengfei Hu, Jiping Li, Zhen Wang, Chen Zhao, Hengxing Ba *, Chunyi Li *

*Institute of Antler Science and Product Technology, Changchun Sci-Tech University, Changchun 130000, China*

ARTICLE INFO

*Keywords:*
Antler reserve mesenchymal cells
miR-143-3p
PRRX1
Extracellular vesicles
Homeostasis
Osteosarcoma
Chondrogenic differentiation

ABSTRACT

The molecular regulation mechanisms for maintaining the homeostasis of mesenchymal stem cells still remains poorly defined. Antler reserve mesenchymal cells (RM cells) persist through the whole rapid antler growth stage as a reserved stem cell population capable of division and differentiation, that makes the RM cells a unique model in stem cell regulation and cancer mechanism studies. Herein, we sequenced and analyzed the extracellular vesicles (EVs) of RM cells in the growth center of antler, and identified a high expression level of miR-143-3p and its target genes IGF1R, TGFβ1, BMP2, etc. The upstream positive regulatory factor PRRX1 of miR-143-3p was identified through ATAC and CUT-taq analysis, combined with dual luciferase assay. We showed that PRRX1 overexpression resulted in a decreased proliferation of RM cells and induced a higher expression of miR-143-3p. miR-143-3p enriched EVs derived from PRRX1 overexpression RM cells had an inhibitory effect on RM cells, osteosarcoma 143B cells (considered as excessive proliferation model for RM cells) and in vivo in osteosarcoma bearing mice, and the mRNA and protein levels of IGF1R were significantly reduced. We confirmed that miR-143-3p enriched EVs inhibited 3D culture induced chondrogenic differentiation of RM cells and xenogeneic antler chondrogenesis through targeting TGFβ1 and BMP2. Together, PRRX1 was identified as an activator of miR-143-3p, and higher amounts of miR-143-3p in EVs of RM cells could inhibit excessive proliferation, and help maintain the undifferentiated state of RM cells. We conclude that PRRX1/miR-143-3p signaling was a regulator of homeostasis of antler RM cells and was a potential regulator of osteosarcoma. Our findings are essential for advancing medical and biological sciences, providing new theoretical foundations and strategies for cancer treatment and tissue regeneration.

## 1. Introduction

The precise regulation of stem cell homeostasis is one of the most important issues in biology. However, there is little research on the paracrine regulation of stem cell homeostasis. The maintenance of stem cell homeostasis is the basis for its long-term existence and functional performance, among which proliferation and differentiation are two important processes of stem cell homeostasis, which are regulated by various factors. While excessive proliferation of stem cells leads to imbalance of tissue and organ homeostasis, further contributes to diseases such as abnormal tissue and organ development, regeneration damage, or tumor occurrence. Currently, there are relevant reports on cell homeostasis maintenance of the brain, liver, and cardiovascular system. For example, one study had shown that a Notch-dependent switch [1] was responsible for a process whereby hindbrain boundary cells underwent neuronal differentiation while maintaining the cell proliferative ability. Another study found that the negative feedback regulatory loop formed by YAP and NR4A1 maintained the balance between cell proliferation and apoptosis [2]. In a further study [3], regulation by cell cycle machinery downstream of the Tmem88-Wnt pathway resulted in a balanced regulation of the proliferation and differentiation processes of progenitor cells in the arch artery. During skin development, denticleless E3 ubiquitin protein ligase (DTL) maintained the proliferation and differentiation of epidermis and hair follicles [4]. The regulatory mechanisms for generating and maintaining stem cell homeostasis, as well as the process of stem cell proliferation and differentiation, are influenced and regulated by multiple factors, and there is a lack of effective animal models for precise studies of molecular regulation.

Deer antler can grow complex bone tissues in a short period of time, makes it as a traditional Chinese medicine and is widely studied, particularly their pharmacological activities [5,6] and clinical

* Corresponding authors.
*E-mail addresses:* bahengxing@cstu.edu.cn (H. Ba), lichunyi1959@163.com (C. Li).

https://doi.org/10.1016/j.ijbiomac.2024.138366
Received 12 September 2024; Received in revised form 29 November 2024; Accepted 2 December 2024

applications [7]. Antler reserve mesenchymal cells (RM cells) at the tip of antler persist during the growth stage as a reserved stem cell population capable of division and differentiation [8–11]. The characteristics of RM cells make it an ideal animal model for the study of cellular homeostasis maintenance [12]. Our previous study showed that RM cells were a kind of PRRX1 positive cell with strong regenerative potential [13]. Through analysis of gene expression during rapid antler growth and of transcriptomics of the antler growth centers at different rates of growth, we have constructed a gene expression regulatory network. We had obtained 55,306 transcripts and 1082 small RNAs related to the rapid growth of antler, among which miR-143-3p were highly expressed in the growth center of deer antler [14]. miR-143 precursor with stem ring structure can be processed into miR-143-3p (the guide strand) and miR-143-5p (the passenger strand) according to different shearing sites. Currently, it had been shown that miR-143-3p had a clear function. Researchers showed that miR-143-3p was closely related to the development of osteosarcoma [7]. Coincidentally, related studies of gene profile had shown that although the growth of antler was very similar to osteosarcoma ($r = 0.67–0.78$), the antler never became cancerous [11]. Therefore, it was hypothesized that antler could serve as a reference model for studying the mechanism of cellular homeostasis, and we speculate that miR-143-3p might be one of the key regulatory factors.

The regulatory mechanism of miR-143-3p is very complex, and it can not only act on multiple target genes, but also work together with other factors. At present, research is focused on functional validation of only a few genes, and the interactions between miR-143-3p and its upstream regulatory factors, as well as between miR-143-3p target genes, are not well understood. In particular, regulation of cellular homeostasis through paracrine pathways needs further exploration as understanding of its regulatory network could provide new avenues for investigation of growth and development and prospects for treatment of disease.

In view of this, we hypothesized that PRRX1/miR-143-3p signaling might regulate the homeostasis of RM cells through paracrine mechanisms. Through multi-omics analysis, in vitro and in vivo studies, the upstream regulatory factor PRRX1 and downstream target gene of miR-143-3p were identified. The EVs of RM cell mediated paracrine pathway were investigated to reveal the regulatory effect of PRRX1/miR-143-3p signaling on the cellular homeostasis of RM cells (Fig. 1). We showed that the high amounts of miR-143-3p in EVs of RM cells could inhibit excessive proliferation and help maintain the undifferentiated state of RM cells, and concluded that PRRX1/miR-143-3p signaling was a regulator of homeostasis in antler RM cells and was a potential regulator of osteosarcoma. In depth research on the mechanisms of RM cell homeostasis, proliferation, and differentiation is essential for advancing medical and biological sciences, providing new theoretical foundations and strategies for cancer treatment and tissue regeneration.

## 2. Results

### 2.1. Expression profile of miRNAs in EVs of antler RM cells

In order to identify the key factors secreted by paracrine pathway that regulates homeostasis of antler RM cells, the miRNA composition in the EVs of antler RM cells were analyzed. Firstly, through isolation and culture of the RM cells in the growth center of deer antler (Fig. 2A), we obtained phenotype stable RM cells that expressed mesenchymal stem cell markers CD73, CD90, NESTIN and specifically expressed COLII (Fig. 2B). The EVs of RM cells were collected (Fig. 2C). After identification, the EVs of RM cells expressed the marker proteins of EVs (Fig. 2D). The particle size of EVs was normal (mean diameter 71.37 ± 19.72 (SD) nm) (Fig. 2E). The expression profile of miRNAs analysis showed that in addition to miRNAs that maintained normal cell growth, miR-143-3p, an important tumor suppressor, was found to be highly expressed (Fig. 2F, Table S1), and as the RM layer gradually differentiated into cartilage, the expression of miR-143-3p was significantly decreased (Fig. 2G). We speculated that miR-143-3p might play an important role in regulating the homeostasis of antler RM cells.

### 2.2. IGF1R was a key target gene of miR-143-3p during the rapid growth of antler

The intersection of differentially expressed genes during the differentiation of antler RM cells (from the RM layer to the pre-cartilage layer and further to the cartilage layer) and the predicted miR-143-3p target genes was obtained; a total of 1422 major candidate target genes of miR-143-3p were identified (Table S2). Subsequently, expression trend analysis and functional enrichment analysis were conducted on these 1422 candidate target genes. We found that the gene expression trend in module 7 was opposite to that of miR-143-3p as evident in Fig. 2G, including IGF1R and other genes highly related to antler growth (Fig. 3A). These target genes were significantly enriched in biological processes of chondrocyte differentiation and positive regulation of cell proliferation (Fig. 3B). We further identified that TGFβ1 and BMP2 (Table S2), which were closely related to chondrocyte differentiation,

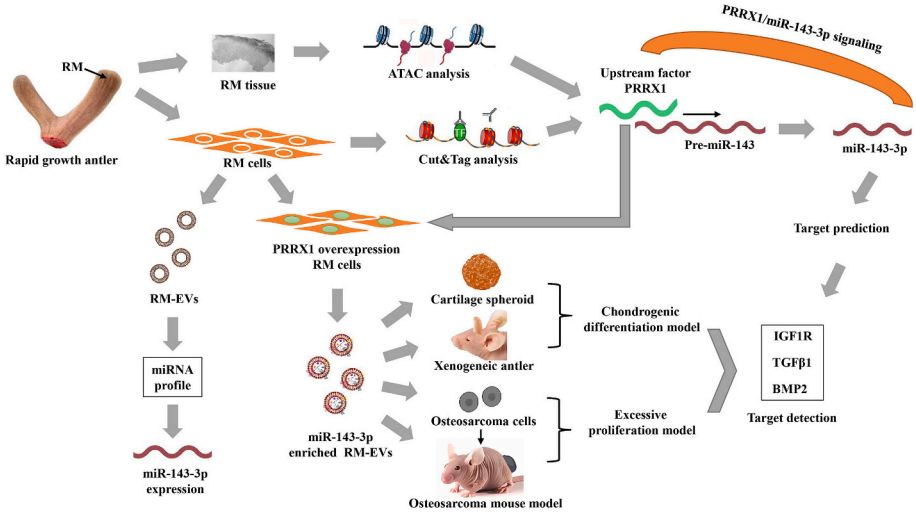


**Fig. 1.** A flowchart summarizing the experimental workflow. We hypothesized that PRRX1/miR-143-3p signaling might regulate the homeostasis of RM cells through paracrine mechanisms. Through multi-omics analysis, in vitro and in vivo studies, the upstream regulatory factor PRRX1 and downstream target gene of miR-143-3p were identified. The EVs of RM cell mediated paracrine pathway were investigated to reveal the regulatory effect of PRRX1/miR-143-3p signaling on the cellular homeostasis of RM cells.

were candidate target genes of miR-143-3p. The results suggested that miR-143-3p might have a function of maintaining the undifferentiated state and inhibiting excessive proliferation of RM cells.

The binding sites of miR-143-3p on the IGF1R mRNA of sika deer were predicted using miRWalk and RNAhybrid software, and two possible binding sites were identified, both located in the CDS region (Fig. 3C). Two wild-type and mutant luciferase reporter plasmids of IGF1R were co-transfected with miR-143 mimic and negative control into 293 T cells. The luciferase activity of the two wild-type groups was significantly reduced compared to mutant groups ($P < 0.01$) (Fig. 3D), indicating that IGF1R was the key target gene of miR-143-3p.

### 2.3. PRRX1 was a regulator of miR-143-3p during the rapid proliferation of antler RM cells

An Assay for Transposase-Accessible Chromatin (ATAC) analysis was performed to determine the upstream regulatory region of pri-miR-143, to predict the regulatory proteins bound to this region, and to identify important factors regulating miR-143-3p expression. The results showed that an ATAC peak was identified around 4 kb upstream of pri-miR-143 (Fig. 4A). A total of 167 transcription factors were predicted to bind to this open region (Table S3), among which 37 transcription factors were differentially expressed in the tissue layers (RM, PC, and CA, three stages of deer antler growth) (Fig. 4B), with PRRX1 being the most significant in terms of differential expression.

The functional enrichment analysis of 37 possible upstream regulatory factors of miR-143-3p showed that the most significant biological function was the negative regulation of cell differentiation (Fig. 4C), suggesting that the transcription factors, such as PRRX1, which inhibit cell differentiation, might be the most critical upstream regulatory factor of miR-143-3p. Further, the protein interaction network analysis of 37 possible upstream regulatory factors of miR-143-3p showed that PRRX1 was a key factor among them (Fig. 4D).

Further validation was conducted at the cellular level using CUT&Tag (Cleavage Under Targets and Tagmentation) to confirm that PRRX1 could bind to the upstream regulatory region of pri-miR-143, which was consistent with the region determined by ATAC seq (Fig. 4A).

The binding ability of transcription factor PRRX1 to the regulatory region of miR-143-3p was validated in 293 T cells using a dual luciferase reporter system. The results showed that when the ATAC peak was missing or mutated, PRRX1 could not bind to the upstream regulatory region of pri-miR-143, and the fluorescence signal was decreased (Fig. 4E). The results further indicated that PRRX1 was a key regulatory factor of miR-143-3p.

### 2.4. Effect of PRRX1-miR-143-3p signaling on the proliferation of RM and osteosarcoma 143B cells

We investigated effect of PRRX1-miR-143-3p signaling on the cell proliferation using RM and osteosarcoma 143B cells. Firstly, we found that the proliferation of RM cells was inhibited after overexpression of PRRX1, while interference with PRRX1 resulted in the opposite effect (Fig. 5A) when compared with the control. The expression levels of miR-143-3p were compared after overexpression and interference of PRRX1. The results showed that overexpression of PRRX1 significantly increased the expression of miR-143-3p, while interference with PRRX1 significantly reduced the expression of miR-143-3p (Fig. 5B), suggesting that the expression of miR-143-3p could be regulated by the expression of PRRX1, thereby changing the proportion of miR-143-3p in the EVs of antler RM cells.

Then, miR-143-3p enriched EVs derived from PRRX1 overexpression RM cells were obtained (miR-143-RM-EVs) (Fig. 5C). The results showed that the number of EVs obtained by the PRRX1 overexpression method was comparable to number of EVs derived from RM cells (Fig. 5D), and the proportion of miR-143-3p in EVs was significantly higher than that of EVs derived from RM cells (Fig. 5E); also the EVs obtained by the two methods all expressed EVs marker proteins (Fig. 5F). Based on these comparisons, this study suggested that the PRRX1 overexpression method could effectively produce miR-143-3p enriched EVs of antler RM cells.

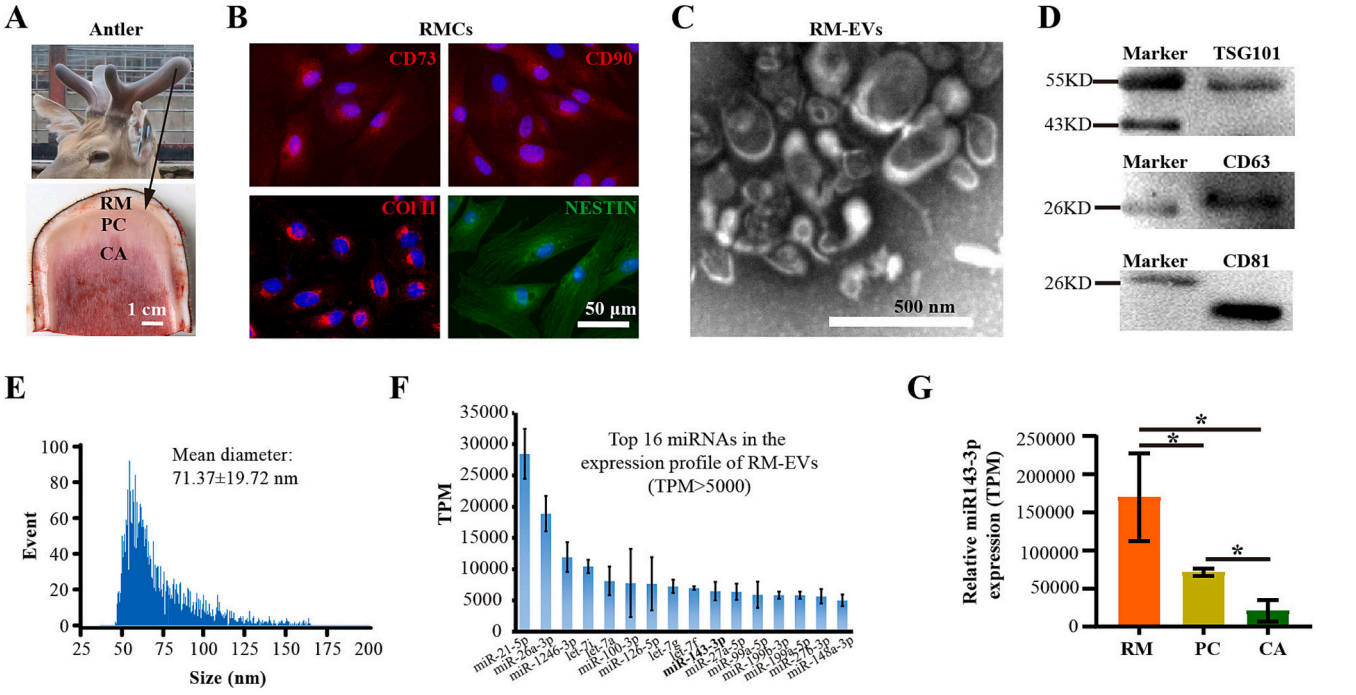


**Fig. 2.** Expression profile of miRNAs in EVs of antler RM cells. A–B, Source and characteristics of the RM cells in the growth center of deer antler for isolation and culture. C, Morphological observation of EVs of RM cells using SEM. D, Western blot identification of the marker proteins of EVs. E, Particle size of RM EVs. F, Expression profile of miRNAs analysis showed that miR-143-3p was highly expressed. G, qPCR analysis of the expression level of miR-143-3p in the RM, PC and CA tissue layers. RM, reserve mesenchyme, PC, pre-cartilage, and CA, cartilage. n = 3, biological replicates per group. *p < 0.05.

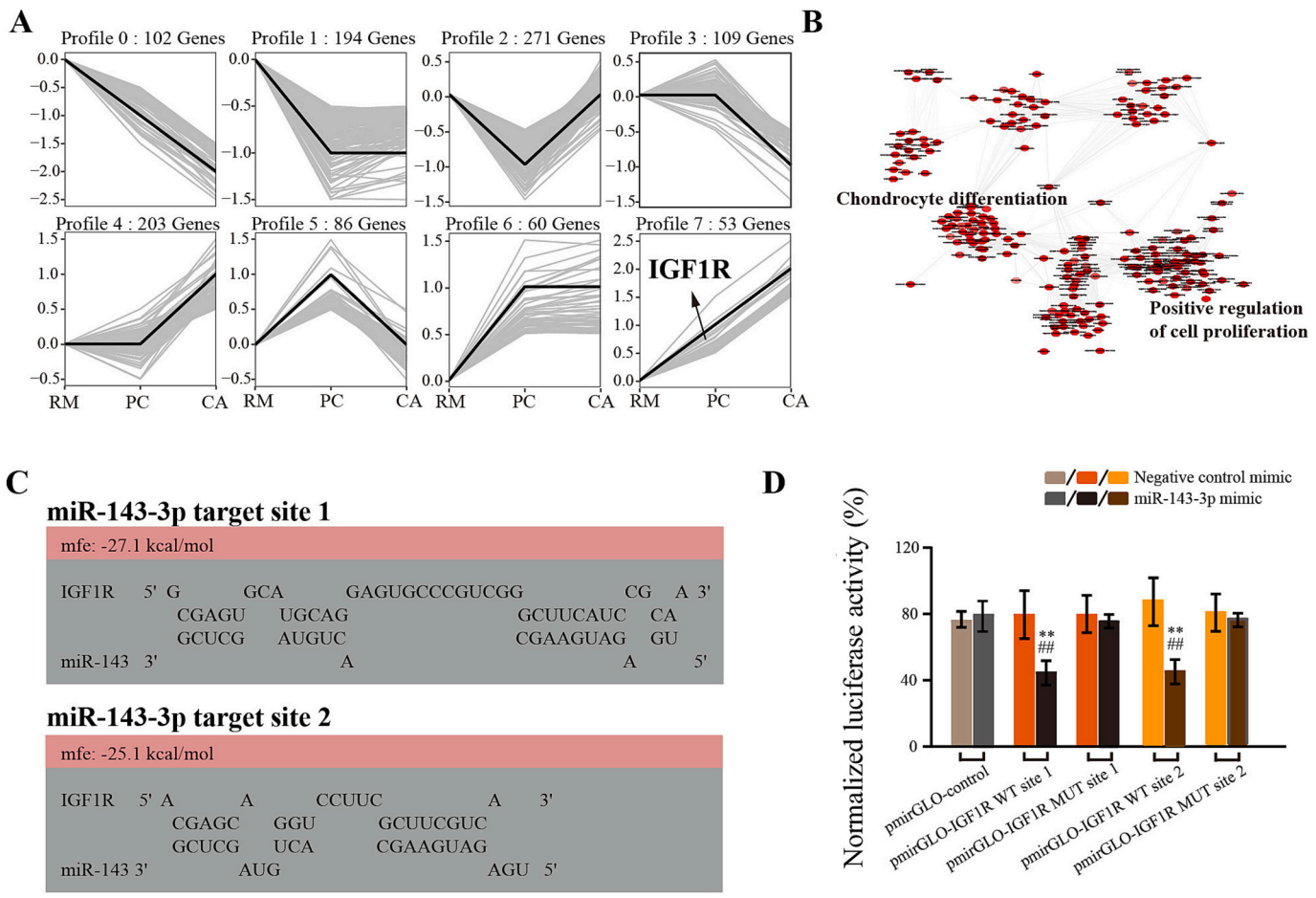


**Fig. 3.** IGF1R was a key target gene of miR-143-3p. A, Through expression trend analysis of the 1422 candidate target genes of miR-143-3p, it was found that the gene expression trend in module 7 was opposite to miR-143-3p, including IGF1R and other genes highly related to antler growth. B, Functional enrichment analysis of the 1422 candidate target genes of miR-143-3p showed that the target genes are significantly enriched in biological processes such as chondrocyte differentiation and positive regulation of cell proliferation. C, The binding sites of miR-143-3p on the IGF1R mRNA of sika deer were predicted using miRWalk and RNAhybrid software, and two possible binding sites were identified, both located in the CDS region. D, Two wild-type and mutant luciferase reporter plasmids of IGF1R were constructed and co-transfected with miR-143 mimic and negative control into 293T cells. The luciferase activity of the two wild-type groups was significantly reduced compared to mutant groups. n = 3 biological replicates per group. $^{**}p < 0.01$ vs pmirGLO-control group; $^{\#\#}p < 0.01$ vs Negative control mimic group.

Subsequently, RM cells were treated with miR-143-RM-EVs, and cell proliferation was inhibited; these effects were confirmed through transfection of miR-143-3p mimics; while transfection of RM cell EVs significantly promoted RM cell proliferation (Fig. 5G). It was speculated that RM EVs contained other factors that promoted RM cell proliferation, while excessive miR-143-3p transported by RM EVs had an inhibitory effect on RM cell proliferation.

Further treatment of 143B cells with miR-143-RM-EVs significantly decreased cell proliferation ability. Transfection of miR-143-3p mimics also confirmed the inhibitory effect of miR-143-3p on 143B cell proliferation, while transfection of RM EVs had no significant effect on 143B cell proliferation (Fig. 5H). Further detection was conducted on the expression of the target gene IGF1R in 143B cells treated with miR-143-RM-EVs. The results showed that the mRNA and protein levels of IGF1R were significantly reduced after treatment (Fig. 5I–J), and the same effect was observed when miR-143-3p mimics were transfected. These results confirm that miR-143-RM-EVs had a significant inhibitory effect on the proliferation of osteosarcoma 143B cells, possibly by reducing the expression of IGF1R. We concluded that the responses of RM cells and 143B cells to PRRX1/miR-143-3p modulation were all suppressed.

### 2.5. *miR-143-3p-enriched-EVs inhibited osteosarcoma in vivo*

Based on the highly similar gene expression pattern of antler and osteosarcoma, we used 143B osteosarcoma as an excessive proliferation model of antler. A 143B osteosarcoma bearing mouse model was constructed to detect the effect of miR-143-3p-enriched-EVs (miR-143-RM-EVs) on 143B osteosarcoma growth.

The results showed that inoculating osteosarcoma 143B cells into the distal femur of nude mice successfully established an in-situ osteosarcoma mouse model (Fig. 6A). Gene expression analysis showed that the expression level of miR-143-3p in 143B cells was extremely low and significantly lower than that in deer antler RM cells (Fig. 6B). The expression level of miR-143-3p in the legs of tumor bearing mice was also significantly lower than that in the leg muscle tissue of normal mice (Fig. 6C). Analysis of the miR-143-3p target gene showed that the expression level of IGF1R in the legs of tumor bearing mice was significantly higher than that in the leg muscle tissue of normal mice (Fig. 6D). miR-143-RM-EVs were injected intratumorally into tumor bearing mice. Two weeks after the treatment, the leg volume and tumor weight of the tumor bearing mice were significantly reduced compared with the control group (Fig. 6E–G), the diameter of the tumors in miR-143-RM-EVs was 0.68 ± 0.15 cm, significantly decreased compared with the control group (1.12 ± 0.07 cm). The target gene IGF1R of miR-143-3p was also significantly inhibited (Fig. 6H–I).

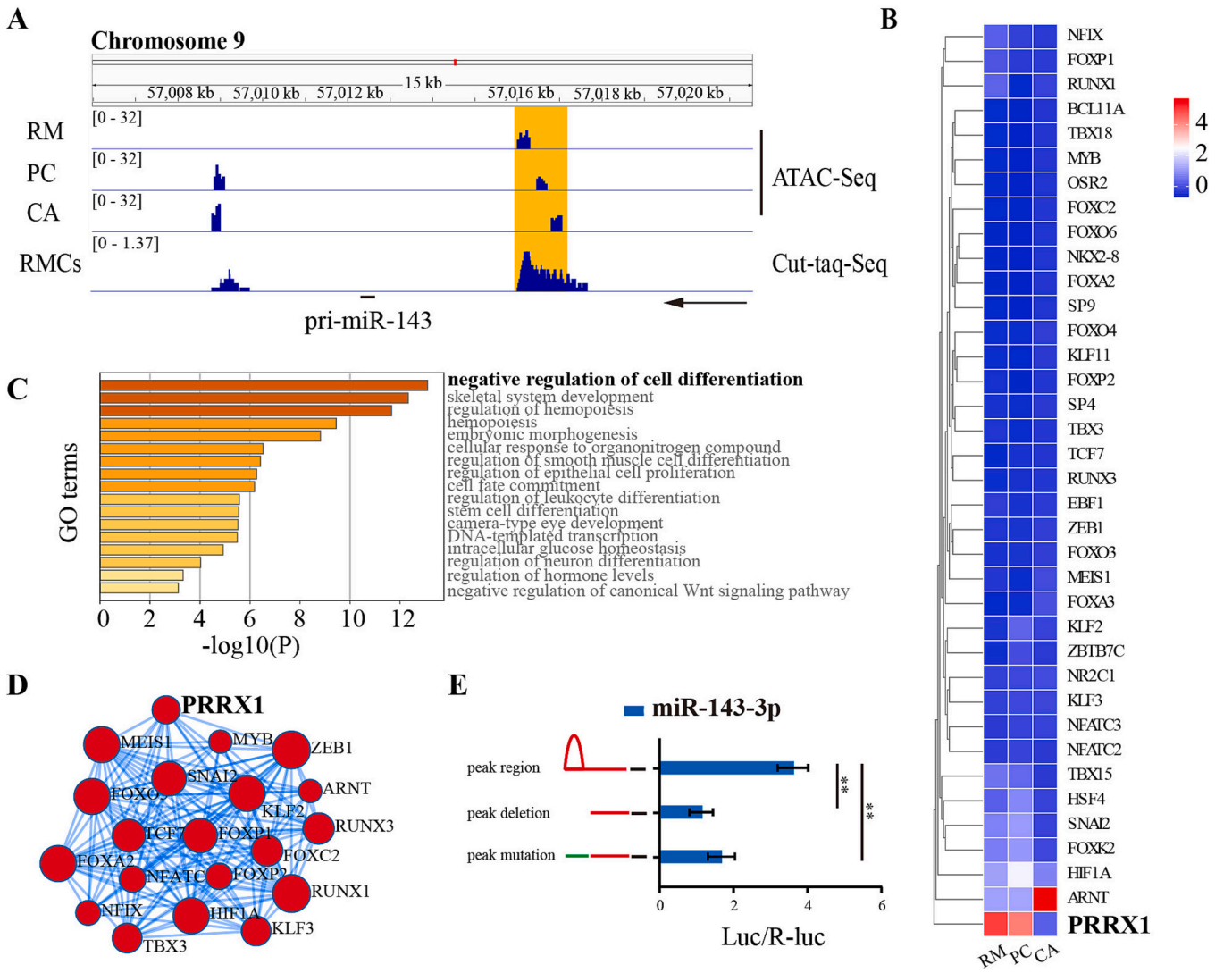


**Fig. 4.** PRRX1 was an upstream factor regulating miR-143-3p expression. A, An ATAC peak was identified around 4kb upstream of pri-miR-143. Validation was conducted at the cellular level using CUT&Tag and confirmed that PRRX1 can bind to the upstream regulatory region of pri-miR-143, which is consistent with the region determined by ATAC seq. B, 37 transcription factors were predicted to bind to the open region of pri-miR-143 and were differentially expressed in the tissue layers (RM, PC, and CA), with PRRX1 being the most significantly differentially expressed. C, The functional enrichment analysis of 37 possible upstream regulatory factors of miR-143-3p showed that the most significant biological function was the negative regulation of cell differentiation. D, The protein interaction network analysis of 37 possible upstream regulatory factors of miR-143-3p showed that PRRX1 is a key factor among them. E, The binding ability of transcription factor PRRX1 to the upstream regulatory region of miR-143-3p was validated in 293T cells using a dual luciferase reporter system. The results showed that when the ATAC peak was missing or mutated, PRRX1 could not bind to the upstream regulatory region of pri-miR-143, and the fluorescence signal was decreased. n = 3 biological replicates per group. **$p < 0.01$.

### *2.6. miR-143-3p-enriched-EVs inhibited chondrogenic differentiation of antler RM cells*

A 3D culture method in antler RM cells without inducing factors (TGFβ1/3) was used to induce chondrogenic differentiation for 21 days; miR-143-RM-EVs were added to the induction system, with the RM-EVs and no EVs groups as controls. The results showed that miR-143-RM-EVs inhibited chondrogenic differentiation of antler RM cells, and could not form spherical structures through the induction period (Fig. 7A); Both the RM-EVs and no EVs groups of RM cells were able to differentiate into cartilage and form spherical structures, which were identified through HE and Alcian Blue staining, and COLII immunofluorescence as spherical structures formed by chondrocyte aggregation (Fig. 7A). The gene and protein expression analysis of three groups showed that the expression of chondrocyte markers TGFβ1 and BMP2 in the miR-143-RM-EVs group was significantly downregulated (Fig. 7B), and TGFβ1 and BMP2 were also candidate target genes of miR-143-3p.

The effect of miR-143-RM-EVs on chondrogenic differentiation at the in vivo level was further validated based on a nude mouse antler model (Fig. 7C). The results showed that the cartilage formation of the nude mouse antler was significantly reduced after administration of miR-143-RM-EVs. Histological observations showed that the tissue formed in the miR-143-RM-EVs group was mainly fibrous connective tissue, while the control group could form cartilage tissue (Fig. 7D). Immunofluorescence analysis showed that the expression of chondrocyte markers TGFβ1 and BMP2 in the nude mice antler of the miR-143-RM-EVs group was significantly downregulated (Fig. 7E–F). These results indicated that miR-143-3p inhibited the chondrogenic differentiation of antler RM cells through targeting TGFβ1 and BMP2 and played an important role in maintaining the undifferentiated state of RM cells during the rapid growth of antler.

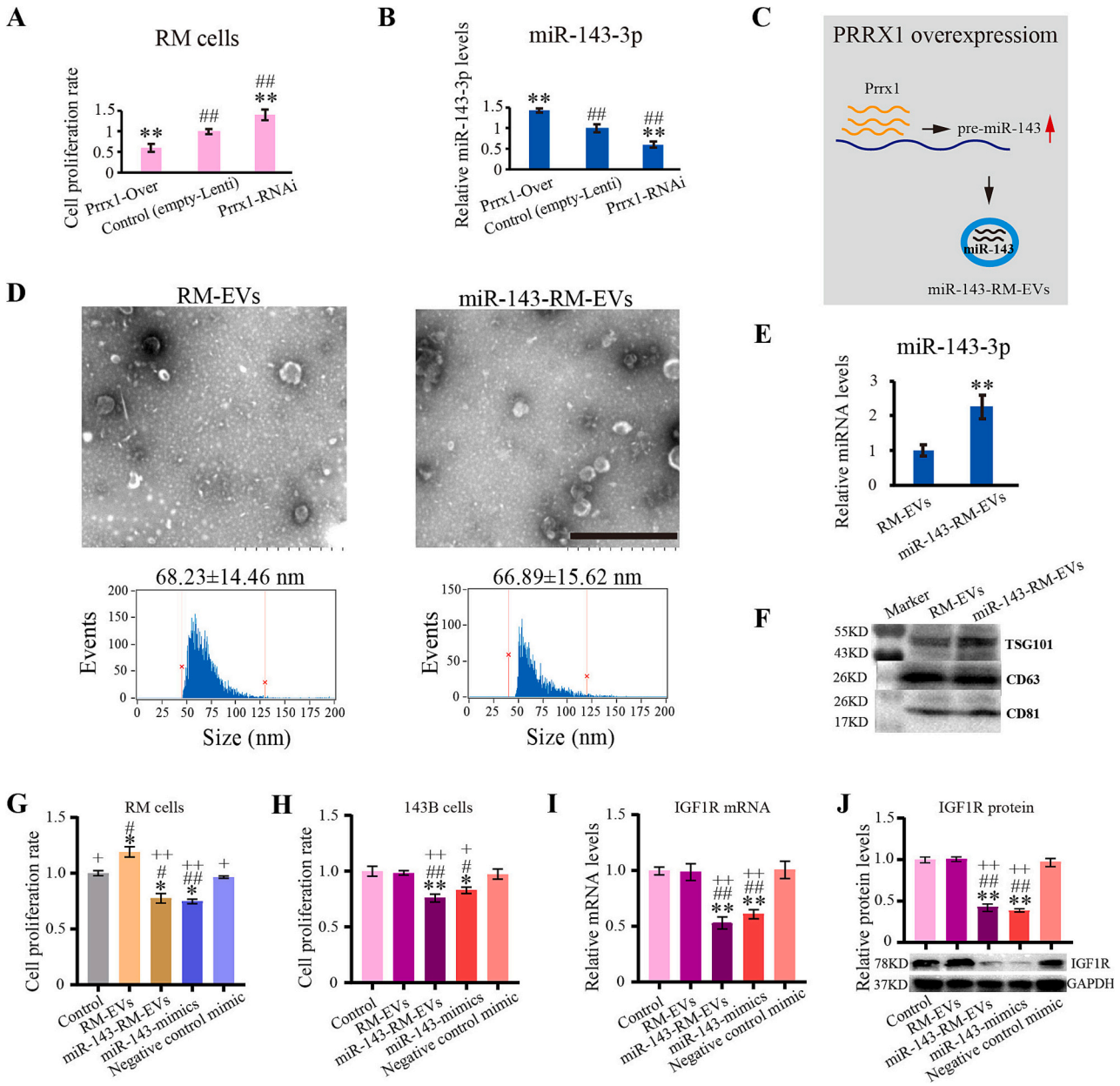


**Fig. 5.** Effect of PRRX1-miR-143-3p signaling on the proliferation of RM and osteosarcoma 143B cells. A, The cell proliferation ability of miR-143-3p was compared after overexpression and interference of PRRX1. $^{**}p < 0.01$ vs control (empty-Lenti) group; $^{\#\#}p < 0.01$ vs Prrx1-Over group. B, The expression levels of miR-143-3p were compared after overexpression of and interference with PRRX1. $^{**}p < 0.01$ vs control (empty-Lenti) group; $^{\#\#}p < 0.01$ vs Prrx1-Over group. C, miR-143-3p enriched EVs were obtained from PRRX1 overexpression antler RM cells. D, The number of EVs obtained by PRRX1 overexpression method. E, The proportion of miR-143-3p in EVs was significantly lower than that of EVs from PRRX1 overexpression RM cells. $^{**}p < 0.01$ vs RM-EVs group. F, The EVs obtained by PRRX1 overexpression method expressed EVs marker proteins. G, RM cells were treated with miR-143-3p enriched EVs, and cell proliferation was inhibited. H, Treatment of 143B cells with miR-143-3p enriched EVs significantly decreased cell proliferation ability. I–J, Detection on the expression of the target gene IGF1R in 143B cells treated with miR-143-3p enriched EVs. The mRNA and protein levels of IGF1R were significantly reduced after treated with miR-143-3p enriched EVs. n = 3, biological replicates per group. $^{*}p < 0.05$ and $^{**}p < 0.01$. G–J: $^{*}p < 0.05$ and $^{**}p < 0.01$ vs Control group; $^{\#}p < 0.05$ and $^{\#\#}p < 0.01$ vs Negative control mimic group; $^{+}p < 0.05$ and $^{++}p < 0.01$ vs RM-EVs group.

## 3. Discussion

In this study, we set out to assess the importance of PRRX1/miR-143-3p signaling in regulating the cellular homeostasis of antler RM cells through paracrine pathways. Studies had shown that miR-143-3p was an anti-cancer factor [15], and its expression was significantly inhibited in osteosarcoma [16]. Through our studies, we elucidated the mechanism by which miR-143-3p derived from EVs of RM cells positively regulated by PRRX1 could inhibit excessive proliferation of antler RM cells through targeting IGF1R and maintain the undifferentiated state of RM cells through targeting TGFβ1 and BMP2 (Fig. 8). This study is important in revealing the paracrine regulatory mechanism for maintenance of the homeostasis state of RM cells, and shows that PRRX1/miR-143-3p signaling might be a potential regulator of osteosarcoma.

The results of this study confirmed that the high expression of miR-143-3p in the EVs of antler RM cells was an inhibitory factor in the regulation of RM cell proliferation and the prevention of carcinogenesis through paracrine pathways in the antler. It has been reported that miR-143-3p plays a regulatory role in various physiological and pathological processes. For example, miR-143-3p could promote wound healing by

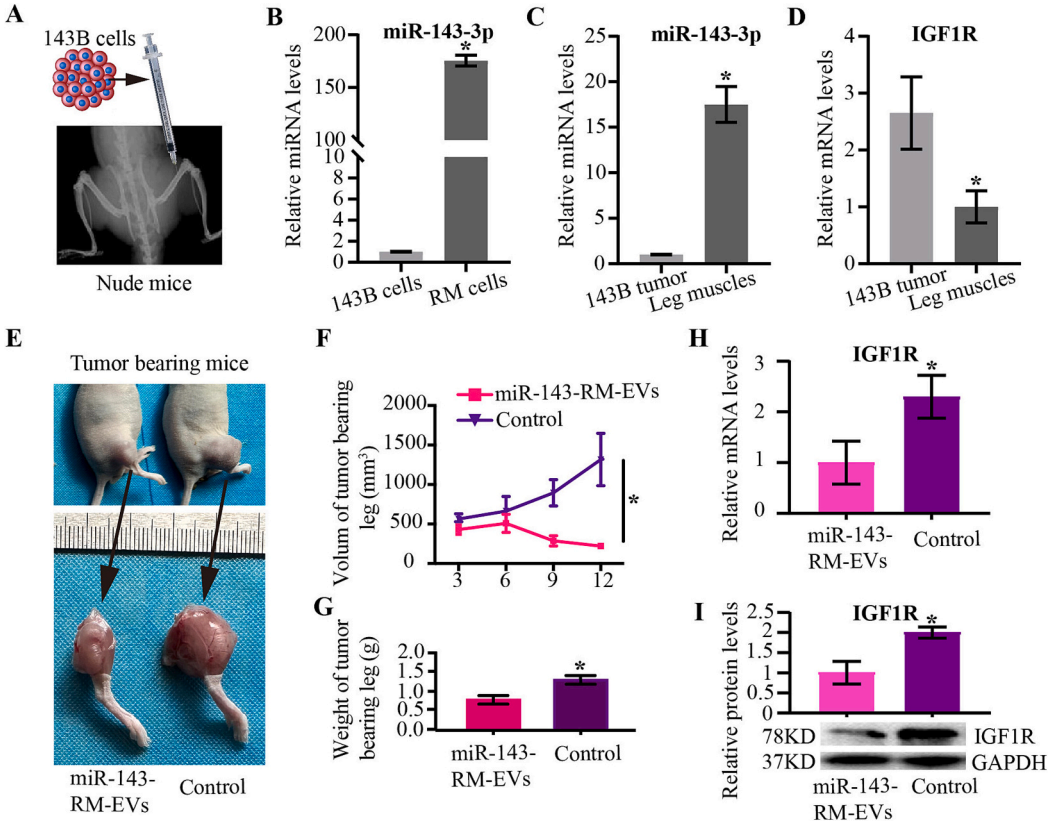


**Fig. 6.** miR-143-3p enriched EVs inhibited osteosarcoma through targeting IGF1R. A, Inoculating osteosarcoma 143B cells into the distal femur of nude mice successfully established an in-situ osteosarcoma mouse model. B, Gene expression analysis showed that the expression level of miR-143-3p in 143B cells was significantly lower than that in deer antler RM cells. C, The expression level of miR-143-3p in the legs of tumor bearing mice was also significantly lower than that in the leg muscle tissue of normal mice. D, Analysis of the miR-143-3p target gene showed that the expression level of IGF1R in the legs of tumor bearing mice was significantly higher than that in the leg muscle tissue of normal mice. E–G, miR-143-3p enriched EVs were injected intratumorally into tumor bearing mice. After 2 weeks of treatment, the leg volume and tumor weight of the tumor bearing mice were significantly lower than those of the control group. H–I, The target gene IGF1R of miR-143-3p was also significantly inhibited in the miR-143-3p enriched EVs group. n = 3 biological replicates per group. *p < 0.05.

regulating IGFBP5 [17,18]; participate in organ formation and development by regulating Notch [19]; and participate in inflammatory response by regulating IL13Rα1 and TLR [20,21]. In addition, miR-143-3p was closely related to the development of tumors [22–25]. The incidence of osteosarcoma was closely related to the decrease of miR-143-3p in vivo. Upregulation of miR-143-3p expression in vitro could significantly reduce the survival ability of osteosarcoma cells and promote cell apoptosis, while upregulation of miR-143-3p expression in osteosarcoma cells in vivo could lead to tumor growth restriction and significant reduction in tumor volume [16]. Further, miR-143-3p could inhibit cell proliferation through interacting with multiple target genes such as KRAS, c-Myc, and ERK5, while in this study, the inhibitory effects of miR-143-3p enriched EVs on proliferation of antler RM cell and 143B osteosarcoma cell were achieved by targeting IGF1R, which involved in cell growth and survival control [26]. The results in this study further demonstrated that miR-143-3p was a tumor suppressor gene [27–29]. However, it would be useful to further compare the responses of RM cells and 143B cells to PRRX1/miR-143-3p modulation in more detail, especially in the differences of gene expression regulation and changes in cell phenotypes.

The results of this study indicated that miR-143-3p not only inhibits RM cell proliferation, but also plays an important role in regulating RM cell differentiation. Other studies have shown that miR-143-3p overexpression inhibited osteogenic differentiation of human adipose-derived mesenchymal stem cells (hADSCs), while miR-143-3p knockdown enhanced this process, and these effects were probably through the k-Ras/MEK/ERK pathway [30]. It was showed that miR-143-3p was downregulated during osteogenic differentiation of dental pulp stem cells (DPSCs), and that miR-143-3p overexpression suppressed osteogenic differentiation of DPSCs [31]. miR-143-3p overexpression could also restrained proliferation and differentiation of bovine skeletal muscle satellite cells (MSCs) through decreasing IGFBP5 [32]. miR-143-3p inhibitors could induce myogenic differentiation of DPSCs [33]. However, there are no reports of miR-143-3p being associated with chondrogenic differentiation. In this study, we have confirmed that miR-143-3p inhibited antler chondrogenic differentiation through targeting TGFβ1 and BMP2, the two factors regulate the growth and differentiation of various cell types [34]. The result in this study further improved the study of miR-143-3p on cell differentiation and confirming that miR-143-3p might be an important regulatory factor in inhibiting cell differentiation.

There is limited research on how miR-143-3p is regulated, and the downregulation of miR-143-3p in cancer is largely unexplained. It has been postulated that epigenetic silencing plays an important regulatory role in miR-143-3p expression. In this respect, it was reported that miR-143-3p was susceptible to DNA demethylation in colorectal cancer (CRC) cells [35]. A DNA methylation study showed that the hypermethylation of pre-miR-143 promoter region resulted in the downregulation of miR-143-3p [36]. In this study, we identified the upstream chromatin open region of pre-miR-143 through ATAC and CUT-taq sequencing, and verified through subsequent experiments that PRRX1 could positively regulate the expression of miR-143-3p. PRRX1 might play a role in homeostasis and regeneration of bone, white adipose tissue and derm [37]. We speculated that PRRX1 could influence the expression of miR-143-3p, probably through chromatin remodeling: Chromatin remodeling regulates miR-143-3p expression by altering the

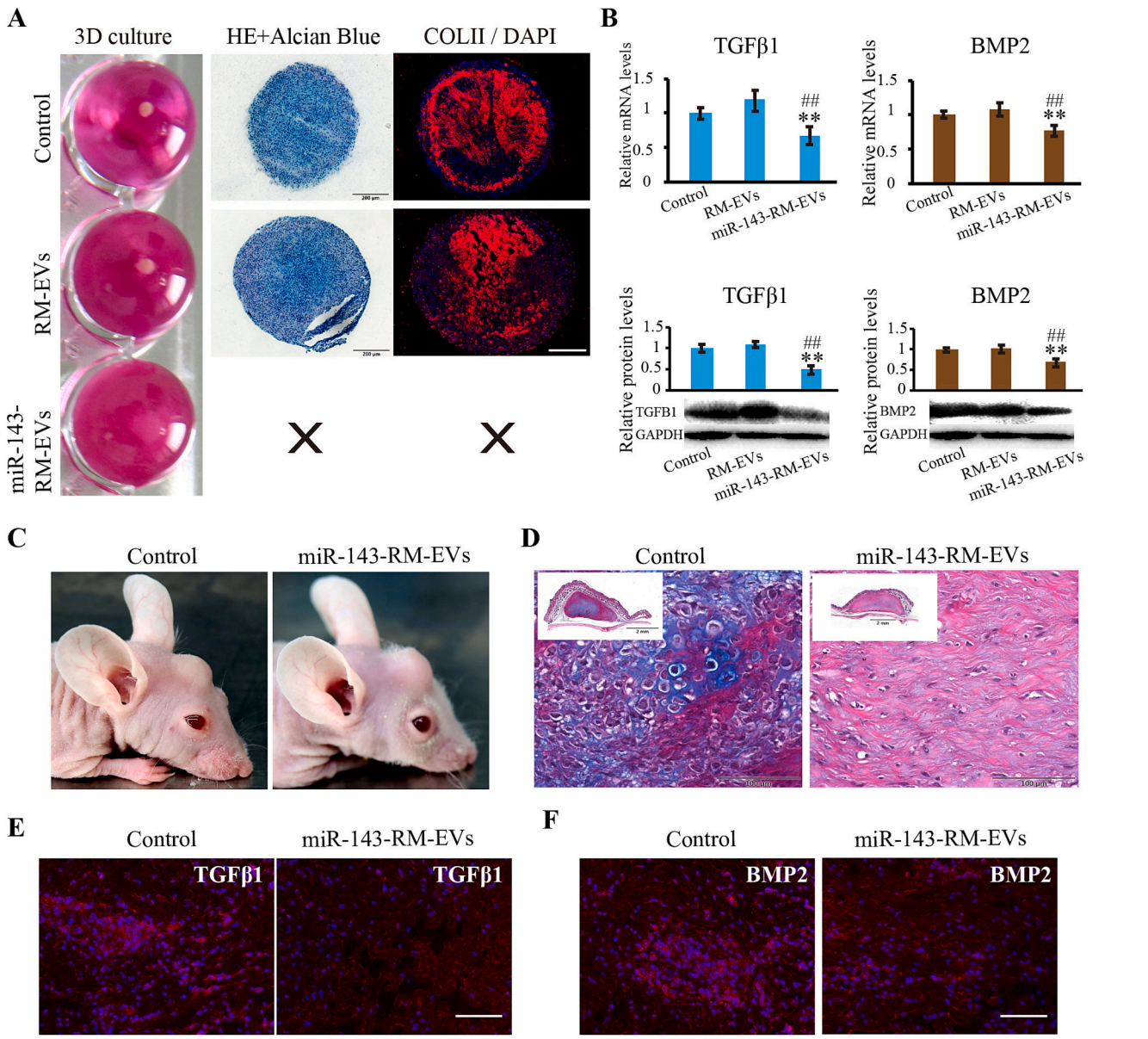


**Fig. 7.** miR-143-3p enriched EVs inhibited antler chondrogenic differentiation through targeting TGFβ1 and BMP2. A, miR-143-3p enriched EVs inhibited chondrogenic differentiation of antler RM cells, and could not form spherical structures throughout the induction period. Both the RM-EVs and no EVs groups of RM cells were able to differentiate into cartilage and form spherical structures, HE and Alcian Blue staining, and COLII immunofluorescence as spherical structures formed by chondrocyte aggregation. B, The gene and protein expression analysis of the expression of chondrocyte markers TGF β 1 and BMP2 in the miR-143-3p enriched EVs group was significantly downregulated. C, The effect of miR-143-3p enriched EVs on chondrogenic differentiation was validated based on a nude mouse antler model. D, Histological observations showed that the tissue formed in the miR-143-3p enriched EVs group was mainly fibrous connective tissue, while the control group could form cartilage tissue. E–F, Immunofluorescence analysis showed that the expression of chondrocyte markers TGF β 1 and BMP2 in the nude mice antler of the miR-143-3p enriched EVs group was significantly downregulated. n = 3, biological replicates per group. $^{**}p < 0.01$ vs Control group; $^{\#\#}p < 0.01$ vs RM-EVs group.

structure and position of chromatin, making it easier for transcription factors to approach and bind to DNA, thereby regulating miR-143-3p transcription. In previous studies, we have shown that PRRX1 served as a marker for antler stem cells [13]. PRRX1 was expressed only in undifferentiated mesenchymal cells and expression gradually ceased with differentiation, indicating that PRRX1 had an inhibitory effect on mesenchymal cell differentiation [38]. Knockout of PRRX1 could promote adipogenesis of MSCs by inhibiting the TGF-β pathway, suggesting that PRRX1 might inhibit adipogenic differentiation of MSCs [39]. In addition, the PRRX1 gene subtype (PRRX1a and PRRX1b) played an important role in cartilage formation. Overexpression of PRRX1a increased pre-cartilage formation and increased chondromas, while overexpression of PRRX1b led to a decrease in them. PRRX1a increased the percentage of cells with proliferative activity in tissue culture and reduced cell apoptosis, while PRRX1b promoted cell apoptosis [40]. It was confirmed that PRRX1a only was expressed during the early stage of chondrogenesis in mesenchymal cells, and high levels of PRRX1b expression occurred during chondrocyte membrane formation [40]. Further research is needed on the genotype of PRRX1 and its role in deer antler regeneration, as well as the systematic time- and dose-dependent regulation of miR-143-3p.

Regulation by paracrine expression played an important role in maintaining tissue and cell homeostasis. Although many attempts have been made to restore expression of miR-143-3p, such as the use of miR-143-3p mimics [41], vesicular stomatitis virus incorporation [42] [43] oncolytic adenovirus [44] and chemical modification [45] [46], these

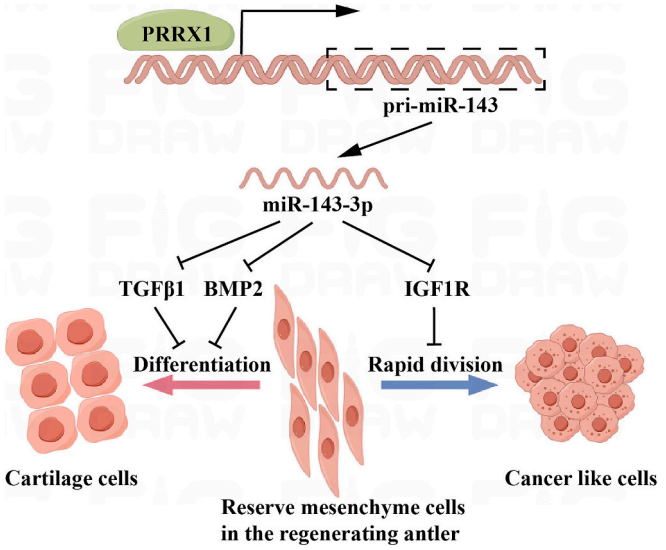


**Fig. 8.** A gene regulatory network centered on PRRX1/miR-143-3p signaling for the regulation of homeostasis of antler RM cells. Based on the results obtained from this study, a gene regulatory network centered on miR-143-3p derived from EVs of antler RM cells was constructed, elucidating the mechanism by which miR-143-3p derived from EVs of RM cells positively regulated by PRRX1 can regulate the homeostasis of antler RM cells by targeting IGF1R to inhibit carcinogenesis, and maintain the undifferentiated state of RM cells by targeting TGF β 1 and BMP2.

methods have proven to be poorly-targeted and less safety. In recent years, the study of miRNA function mediated by EVs had attracted widespread attention [47–49]. In this study we showed that the microRNA enriched EVs were efficient vehicles for transporting miRNA to exert its biological functions, although further work is needed to compare the loading efficiency of different methods. However, the method of loading EVs with miRNA has significant advantages compared to other methods, and the complex mechanisms of EVs-mediated cellular communication and its regulation of cellular homeostasis still require further research.

Deer antler is a unique model to study the regulation of rapid organ regeneration and cancer mechanisms [50], the applicability of results found in antler to different models still need verification. However, based on mammals, the key factors and their pathways and mechanisms in deer antler have important reference significance for human organ regeneration, tissue repair, and cancer research.

We employ multi-omics approaches (ATAC and CUT-taq analysis), and use multi-level experimental designs (in vitro and in vivo studies), and highlight the involvement of EVs in mediating paracrine signaling. Which could more comprehensively reveal the regulation of PRRX1/miR-143-3p signaling on proliferation and differentiation. These findings suggest that this pathway may play a significant role in maintaining cellular balance and could have potential implications for understanding osteosarcoma regulation. The manuscript contributes valuable data to the field of stem cell and cancer biology by elucidating a novel PRRX1/miR-143-3p axis in RM cell regulation, and these comprehensive approaches strengthen the conclusions and enhance the study's validity.

In summary, the present results are significant in at least two major respects. Firstly, we identified the upstream chromatin open region of pre-miR-143 through ATAC and CUT-taq analysis, and verified through subsequent experiments that PRRX1 could positively regulate the expression of miR-143-3p; Secondly, we showed that the paracrine pathway mediates the regulatory effect of PRRX1/miR-143-3p signaling on the proliferation and chondrogenic differentiation of RM cells, as well as the excessive proliferation of osteosarcoma 143B cells. This study provides a basis for exploring the paracrine regulation mechanism by which cell populations maintain homeostasis through PRRX1/miR-143-3p signaling.

## 4. Materials and methods

### 4.1. Ethical statement

All animal experiments were carried out in accordance with the National Research Council's Guide for the Care and Use of Laboratory Animals. All procedures concerning animals were approved by the Institutional Animal Ethics Committee of Changchun Sci-Tech University, Changchun, China (Ethics No.: CKARI202323).

### 4.2. Isolation and in vitro culture of RM cells

Deer antlers were provided by Jilin Dongao Deer Industry Group Co. Ltd. The RM cells were isolated from antler RM tissue in rapid growth stage using the method preciously reported [9], fresh deer antler tissue was shaved with surgical blades, and disinfected with iodine and 75 % alcohol, then used a surgical knife to cut RM tissue and removed connective tissue, cut into small pieces and transferred to a mixture of type I collagenase (200 U/mL, Gibco, 9001-12-1) and type II collagenase (150 U/mL, Gibco, 17,101–015), digested at 37 °C for 15 min and centrifuged at 1000 r/min to remove collagenase, transferred the chopped tissue pieces to a culture dish and disperse them, added a small amount of culture medium to make the tissue pieces adhere to the wall, and placed them in a carbon dioxide incubator, changed the culture medium every 2 days and continued culturing until the RM cells migrated out. The RM cells were cultured in complete medium containing 89 % DMEM, 10 % fetal bovine serum and 1 % penicillin/streptomycin (100×) at 37 °C $CO_2$ incubator. The RM cells in the logarithmic phase of growth were used for isolation of the EVs.

### 4.3. Isolation and characterization of EVs

The RM cells were cultured for 48 h in DMEM medium containing 10 % exosome free fetal bovine serum, then the supernatant was collected and EVs released from RM cells were obtained using gradient centrifugation method, namely the collected cell culture medium was centrifuged at 300 g, 2000 g, and 10,000 g to remove cell debris and large molecular proteins, and finally centrifuged at 100000 g to obtain RM EVs. The morphology analysis of EVs was carried out by transmission electron microscopy (TEM; Hitachi H7650, Japan). The size and concentration of EVs were characterized by nanoflow cytometry (NanoFCM). EV markers such as TSG101, CD81 and CD63 were detected by western blot analysis.

### 4.4. MicroRNA analysis of EVs

EVs were used for RNA extraction, RNA degradation, purity and integrity were checked subsequently. microRNAs (miRNAs) were sequenced on a novaseq 6000 platform (Novogene Co., LTD, China). The known miRNAs were identified by comparison against miRNA precursor sequences from miRBase22.0 using mirDeep2 software. Differentially expressed miRNAs were identified using DEGsEq. (1.38.0) R package, P value $<0.05$ and $|\log2(\text{foldchange})| > 1$ was set as filters.

### 4.5. miRNA targets prediction, functional enrichment analysis

Targets of miRNAs were predicted by RNAhybrid 2.2 software. The functional enrichment analysis was carried out using Metascape software.

### 4.6. Luciferase activity assay of miRNA binding sites

Recombinant pmir-GLO luciferase plasmid were constructed using wild-type/mutated miRNA binding sequence amplified from deer IGF1R

gene. The constructed plasmid, together with miR-143-3p mimic or negative control mimic were co-transfected to 293 T cells using Lipofectamine 3000 (Invitrogen, USA). After 24 h culture, luciferase activity was analyzed using the Spark multimode microplate reader (TECAN, Austria). Three individual experiments were performed for statistical purposes. Primers were listed in Tables S4.

### 4.7. ATAC analysis of miRNA upstream region and enrichment analysis of region-associated genes

ATAC data were obtained from our previous published studies which deposited in Genome Sequence Archive in National Genomics Data Center (https://ngdc.cncb.ac.cn/gsa) with accession number CRA014751. Peak region was defined using MACS2 v2.1.1 software. The genes associated within the peak region were annotated and used for enrichment analysis using Metascape database.

### 4.8. PRRX1-CUT&Tag analysis of miRNA upstream region and verified through luciferase activity assay

PRRX1-CUT&Tag data of RM cells was obtained from our previous data deposited in Genome Sequence Archive in National Genomics Data Center with accession number CRA014775. all peak regions were defined using MACS2 software and annotated using ChIPseeker software. pGL3.0 plasmid containing fragments of wild, mutated and deleted peak regions of miR-143-3p were constructed, respectively, and co-transfected with pCDNA3.1-PRRX1 and phRL-TK plasmids into 293 T cells. After 24 h of transfection, luciferase signaling was detected using fluorescence spectrophotometer. Primer information were listed in Table S4.

### 4.9. PRRX1 overexpression and RNAi RM cells

Three groups, namely PRRX1 overexpression RM cells, PRRX1 RNAi RM cells, and empty lentiviral vector infected RM cells were used to detect cell proliferation rate and miR-143-3p expression levels, these cells were constructed in our previous study and preserved in our laboratory. EVs released from PRRX1 overexpression RM cells were also collected to detect miR-143-3p expression. Primers for microRNAs were designed by stem loop methods (Table S4). U6 were used as internal reference. Each group has 3 biological replicates, respectively.

### 4.10. The responses of RM cells and 143B cells to PRRX1/miR-143-3p modulation

The RM and 143B cells were seeded into 96/6 well plates at a concentration of $3000/10^5$ cells per well, respectively, and treated with four groups of EVs and miRNA mimics for 24 h, namely RM-EVs group, miR-143-RM-EVs group, miR-143 mimics group, negative mimics control group and control group with no EVs or mimics treatment. Then the cells were collected for CCK-8 (Apexbio, K1018), quantitative real-time PCR and western blot analysis according to the instruction manual. Each group has three biological replicates, respectively.

### 4.11. Quantitative real-time PCR analysis

RNA was extracted using TRIZOL (Thermo Fisher, USA), RNA concentration was determined by Micro spectrophotometer (Nano-300, Aosheng, China); cDNA synthesis was carried out using PrimeScript RT Master Mix kit (Takara, Japan); Gene expression were quantified using SYBR Premix EX Taq (Perfect Real time) (Takara, Japan) on a quantitative real-time PCR system (qTOWER3G, Germany). Three individual experiments were performed for statistical purposes. The results were analyzed using the $2^{-\triangle\triangle CT}$ method.

### 4.12. Western blot analysis

Tissue or cells were used for protein extraction using RIPA solution (Sigma, USA). Phenylmethanesulfonyl fluoride (PMSF) and protease/phosphatase inhibitors were added during the extraction process to avoid protein degradation. Protein concentrations were assessed using BCA protein assay kit (ZJ101, EpiZyme, China). Protein quantity was then analyzed through SDS–PAGE electrophoresis, transmembrane, primary-second antibody incubation and chemiluminescence. The relative quantity of Rabbit Anti-GAPDH antibody (bs-2188R) served as control. The primary antibodies were Rabbit Anti-BMP2 antibody (bs-0514R), Rabbit Anti-TGF beta 1 antibody (bs-0086R), Rabbit Anti-IGF1R antibody (bs-0227R), respectively.

### 4.13. Construction of osteosarcoma orthotopic model

4-week old female Balb/c nude mice were selected and injected with 143B cells to establish osteosarcoma orthotopic model. In total, 6 tumor bearing nude mice were randomly divided into two groups (3 mice/group): Control, miR-143-RM-EVs group. The miR-143-RM-EVs were intratumorally injected every 2 days for 6 times; The control group received 200 μL saline. The tumor volume was measured every other day during treatment. At the end of treatment, mice were anesthetized and the tumor was removed, photographed, weighed, and prepared for qPCR and WB assessment.

### 4.14. Chondrogenic differentiation and miR-143-RM-EVs treatment

The RM cells were seeded into Nunclon Sphera 3D Culture System at a density of $2 \times 10^4$ cells/well, and divided into three groups (12 well/group): Control, RM-EVs group, miR-143-RM-EVs group. The formation and growth of spheroids were analyzed at 21 days using the frozen section, with alcian blue staining, immunofluorescence analysis, qPCR and WB analysis.

### 4.15. Xenogeneic antler mouse model treated with miR-143-RM-EVs

Xenogeneic antler model were constructed according to method previous reported [51], and divided into two groups (three mouse/group): Control, miR-143-RM-EVs group. In the miR-143-RM-EVs group, miR-143-RM-EVs ($10^8$ EVs/mouse) were injected into the xenogeneic antlers, with 2–3 injections per week for 3 weeks, the control group received 200 μL saline. The xenogeneic antler samples were taken at 21 days of transplantation from anesthetized mice. Analyses of the xenogeneic antlers were carried out with HE-Alcian blue staining, immunofluorescence analysis, respectively.

### 4.16. Statistical analysis

The treatment conditions (such as timing, concentration, and intervention frequency) were consistent between each group in cell and animal experiments. Two-tailed Student's t-text was used to compare the differences between two groups. One-way ANOVA and post hoc Bonferroni tests were used to compare differences among more than two groups. Significant differences were considered when $p < 0.05$.

Supplementary data to this article can be found online at https://doi.org/10.1016/j.ijbiomac.2024.138366.

## CRediT authorship contribution statement

**Pengfei Hu:** Writing – original draft, Visualization, Validation, Software, Resources, Project administration, Methodology, Investigation, Funding acquisition, Formal analysis, Data curation, Conceptualization. **Jiping Li:** Methodology, Investigation. **Zhen Wang:** Resources, Methodology, Investigation. **Chen Zhao:** Resources, Methodology. **Hengxing Ba:** Writing – review & editing, Supervision. **Chunyi Li:**

Writing – review & editing, Supervision.

## Ethics approval and consent to participate

All animal experiments were carried out in accordance with the National Research Council's Guide for the Care and Use of Laboratory Animals. All procedures concerning animals were approved by the Institutional Animal Ethics Committee of Changchun Sci-Tech University, Changchun, China (Ethics No.: CKARI202323).

## Consent for publication

Not applicable.

## Funding

This research was funded by the National Natural Science Foundation of China (U23A20523, U20A20403), the Natural Science Foundation of Jilin Province (No. YDZJ202101ZYTS102, YDZJ202201ZYTS690), and the Doctoral Research Start-Up Fund of Changchun Sci-Tech University (202306).

## Declaration of competing interest

The authors declare that they have no known competing financial interests or personal relationships that could have appeared to influence the work reported in this paper.

## Acknowledgments

The authors thank Peter Fennessy for polishing the English.

## Data availability

The raw sequencing data reported in this paper have been deposited in the Genome Sequence Archive in National Genomics Data Center, China National Center for Bioinformation/Beijing Institute of Genomics, Chinese Academy of Sciences (miRNA-seq: CRA015784; ATAC-seq: CRA014751; Prrx1-CUT&Tag-Seq: CRA014775) that are publicly accessible at https://ngdc.cncb.ac.cn/gsa.

## References

[1] C.F. Hevia, C. Engel-Pizcueta, F. Udina, C. Pujades, The neurogenic fate of the hindbrain boundaries relies on Notch3-dependent asymmetric cell divisions, Cell Rep. 39 (2022) 110915.
[2] L. He, L. Yuan, W. Yu, Y. Sun, D. Jiang, X. Wang, et al., A regulation loop between YAP and NR4A1 balances cell proliferation and apoptosis, Cell Rep. 33 (2020) 108284.
[3] M. Zhang, J. Liu, A. Mao, G. Ning, Y. Cao, W. Zhang, et al., Tmem88 confines ectodermal Wnt2bb signaling in pharyngeal arch artery progenitors for balancing cell cycle progression and cell fate decision, Nature Cardiovascular Research 2 (2023) 234–250.
[4] Y. Lin, W. Tang, P. Huang, Z. Wang, L. Duan, C. Jia, et al., Denticleless E3 ubiquitin protein ligase (DTL) maintains the proliferation and differentiation of epidermis and hair follicles during skin development, Dev. Dyn. 253 (2024) 635–647.
[5] X. Rong, W. Chu, H. Zhang, Y. Wang, X. Qi, G. Zhang, et al., Antler stem cell-conditioned medium stimulates regenerative wound healing in rats, Stem Cell Res Ther 10 (2019) 019–1457.
[6] G. Zhang, L. Shi, J. Li, S. Wang, J. Ren, D. Wang, et al., Antler stem cell exosomes alleviate pulmonary fibrosis via inhibiting recruitment of monocyte macrophage, rather than polarization of M2 macrophages in mice, Cell Death Dis. 9 (2023) 023–01659.
[7] J. Lei, X. Jiang, W. Li, J. Ren, D. Wang, Z. Ji, et al., Exosomes from antler stem cells alleviate mesenchymal stem cell senescence and osteoarthritis, Protein & Cell 13 (2022) 220–226.
[8] J.S. Price, B.O. Oyajobi, R.O. Oreffo, R.G. Russell, Cells cultured from the growing tip of red deer antler express alkaline phosphatase and proliferate in response to insulin-like growth factor-I, J. Endocrinol. 143 (1994).
[9] C. Li, D.E. Clark, E.A. Lord, J.A. Stanton, J.M. Suttie, Sampling technique to discriminate the different tissue layers of growing antler tips for gene discovery, Anat. Rec. 268 (2002) 125–130.
[10] D.E. Clark, C. Li, W. Wang, S.K. Martin, J.M. Suttie, Vascular localization and proliferation in the growing tip of the deer antler, Anat Rec A Discov Mol Cell Evol Biol 288 (2006) 973–981.
[11] Y. Wang, C. Zhang, N. Wang, Z. Li, R. Heller, R. Liu, et al., Genetic basis of ruminant headgear and rapid antler regeneration, Science 364 (2019).
[12] D. Wang, D. Berg, H. Ba, H. Sun, Z. Wang, C. Li, Deer antler stem cells are a novel type of cells that sustain full regeneration of a mammalian organ-deer antler, Cell Death Dis. 10 (2019) 019–1686.
[13] T. Qin, G. Zhang, Y. Zheng, S. Li, Y. Yuan, Q. Li, et al., A population of stem cells with strong regenerative potential discovered in deer antlers, Science 379 (2023) 840–847.
[14] P. Hu, T. Wang, H. Liu, J. Xu, L. Wang, P. Zhao, et al., Full-length transcriptome and microRNA sequencing reveal the specific gene-regulation network of velvet antler in sika deer with extremely different velvet antler weight, Mol. Gen. Genomics. 294 (2019) 431–443.
[15] B. Wang, Y. Xu, Y. Wei, L. Lv, N. Liu, R. Lin, et al., Human mesenchymal stem cell-derived exosomal microRNA-143 promotes apoptosis and suppresses cell growth in pancreatic cancer via target gene regulation, Front. Genet. (2021) 12.
[16] W.H. Li, H.J. Wu, Y.X. Li, H.G. Pan, T. Meng, X. Wang, MicroRNA-143 promotes apoptosis of osteosarcoma cells by caspase-3 activation via targeting Bcl-2, Biomed. Pharmacother. 80 (2016) 8–15.
[17] A. Soriano-Arroquia, R. McCormick, A.P. Molloy, A. McArdle, K. Goljanek-Whysall, Age-related changes in miR-143-3p:Igfbp5 interactions affect muscle regeneration, Aging Cell 15 (2016) 361–369.
[18] R.R. Chivukula, G. Shi, A. Acharya, E.W. Mills, L.R. Zeitels, J.L. Anandam, et al., An essential mesenchymal function for miR-143/145 in intestinal epithelial regeneration, Cell 157 (2014) 1104–1116.
[19] N. Rani, T.J. Nowakowski, H. Zhou, S.E. Godshalk, V. Lisi, A.R. Kriegstein, et al., A primate lncRNA mediates Notch signaling during neuronal development by sequestering miRNA, Neuron 90 (2016) 1174–1188.
[20] Y. Teng, R. Zhang, C. Liu, L. Zhou, H. Wang, W. Zhuang, et al., miR-143 inhibits interleukin-13-induced inflammatory cytokine and mucus production in nasal epithelial cells from allergic rhinitis patients by targeting IL13Rα1, Biochem. Biophys. Res. Commun. 457 (2015) 58–64.
[21] X. Xia, Z. Li, K. Liu, Y. Wu, D. Jiang, Y. Lai, Staphylococcal LTA-induced miR-143 inhibits Propionibacterium acnes-mediated inflammatory response in skin, J Invest Dermatol 136 (2016) 621–630.
[22] F. Li, Y. Han, R. Chen, Y. Jiang, C. Chen, X. Wang, et al., MicroRNA-143 acts as a tumor suppressor through Musashi-2/DLL1/Notch1 and Musashi-2/Snail1/MMPs axes in acute myeloid leukemia, J. Transl. Med. 21 (2023) 023–04106.
[23] V. Asghariazar, B. Mansoori, M. Kadkhodayi, E. Safarzadeh, A. Mohammadi, B. Baradaran, et al., MicroRNA-143 act as a tumor suppressor microRNA in human lung cancer cells by inhibiting cell proliferation, invasion, and migration, Mol. Biol. Rep. 49 (2022) 7637–7647.
[24] V. Asghariazar, M. Kadkhodayi, B. Mansoori, A. Mohammadi, B. Baradaran, Restoration of miR-143 reduces migration and proliferation of bladder cancer cells by regulating signaling pathways involved in EMT, Mol. Cell. Probes 61 (2022) 2.
[25] N. Hosseinahli, T. Zeinali, L. Karimi, D. Shanehbandi, B. Mansoori, A. Mohammadi, et al., Restoration of miRNA-143 expression inhibits growth and migration of MKN-45 gastric cancer cell line, Adv Pharm Bull 12 (2022) 183–190.
[26] G. Pandini, F. Frasca, R. Mineo, L. Sciacca, R. Vigneri, A. Belfiore, Insulin/insulin-like growth factor I hybrid receptors have different biological characteristics depending on the insulin receptor isoform involved, J. Biol. Chem. 277 (2002) 39684–39695.
[27] C. Clapé, V. Fritz, C. Henriquet, F. Apparailly, P.L. Fernandez, F. Iborra, et al., miR-143 interferes with ERK5 signaling, and abrogates prostate cancer progression in mice, PLoS One 4 (2009) 0007542.
[28] X. Chen, X. Guo, H. Zhang, Y. Xiang, J. Chen, Y. Yin, et al., Role of miR-143 targeting KRAS in colorectal tumorigenesis, Oncogene 28 (2009) 1385–1392.
[29] H. Zhang, X. Cai, Y. Wang, H. Tang, D. Tong, F. Ji, microRNA-143, down-regulated in osteosarcoma, promotes apoptosis and suppresses tumorigenicity by targeting Bcl-2, Oncol. Rep. 24 (2010) 1363–1369.
[30] Y. Zhang, K. Zhou, L. Wu, H. Gu, Z. Huang, J. Xu, Downregulation of microRNA-143 promotes osteogenic differentiation of human adipose-derived mesenchymal stem cells through the k-Ras/MEK/ERK signaling pathway, Int. J. Mol. Med. 46 (2020) 965–976.
[31] P. Zhang, W. Yang, G. Wang, Y. Li, miR-143 suppresses the osteogenic differentiation of dental pulp stem cells by inactivation of NF-κB signaling pathway via targeting TNF-α, Arch. Oral Biol. 87 (2018) 172–179.
[32] W.R. Zhang, H.N. Zhang, Y.M. Wang, Y. Dai, X.F. Liu, X. Li, et al., miR-143 regulates proliferation and differentiation of bovine skeletal muscle satellite cells by targeting IGFBP5, In Vitro Cell Dev Biol Anim 53 (2017) 265–271.
[33] D. Li, T. Deng, H. Li, Y. Li, MiR-143 and miR-135 inhibitors treatment induces skeletal myogenic differentiation of human adult dental pulp stem cells, Arch. Oral Biol. 60 (2015) 1613–1617.
[34] N.J. Kovermann, V. Basoli, E. Della Bella, M. Alini, C. Lischer, H. Schmal, et al., BMP2 and TGF-β cooperate differently during synovial-derived stem-cell chondrogenesis in a dexamethasone-dependent manner, Cells (2019) 8.
[35] A. Omar, D. Govan, C. Penny, Epigenetic regulation in colorectal cancer: the susceptibility of microRNAs 145, 143 and 133b to DNA demethylation and histone deacetylase inhibitors, PLoS One 18 (2023).
[36] W.Y. Chen, Z.Q. Lang, C. Ren, P. Yang, B. Zhang, miR-143 acts as a novel Big mitogen-activated protein kinase 1 suppressor and may inhibit invasion of glioma, Oncol. Rep. 42 (2019) 1194–1204.

[37] H. Liu, P. Li, S. Zhang, J. Xiang, R. Yang, J. Liu, et al., Prrx1 marks stem cells for bone, white adipose tissue and dermis in adult mice, Nat. Genet. 54 (2022) 1946–1958.
[38] M.F. Lu, H.T. Cheng, M.J. Kern, S.S. Potter, B. Tran, T.G. Diekwisch, et al., prx-1 functions cooperatively with another paired-related homeobox gene, prx-2, to maintain cell fates within the craniofacial mesenchyme, Development 126 (1999) 495–504.
[39] B. Du, W.P. Cawthorn, A. Su, C.R. Doucette, Y. Yao, N. Hemati, et al., The transcription factor paired-related homeobox 1 (Prrx1) inhibits adipogenesis by activating transforming growth factor-β (TGFβ) signaling, J. Biol. Chem. 288 (2013) 3036–3047.
[40] R.E. Peterson, S. Hoffman, M.J. Kern, Opposing roles of two isoforms of the Prx1 homeobox gene in chondrogenesis, Dev. Dyn. 233 (2005) 811–821.
[41] A.A. Farooqi, M.Z. Qureshi, R. Attar, S.S. Alhewairini, S. Fayyaz, U. Y. Sabitaliyevich, et al., MicroRNA-143 as a new weapon against cancer: overview of the mechanistic insights and long non-coding RNA mediated regulation of miRNA-143 in different cancers, Cell. Mol. Biol. 65 (2019) 1–5.
[42] T. Sakuda, T. Kubo, M.P. Johan, T. Furuta, T. Sakaguchi, N. Adachi, Development of an oncolytic recombinant vesicular stomatitis virus encoding a tumor-suppressor microRNA, Anticancer Res. 40 (2020) 6319–6325.
[43] T. Sakuda, T. Kubo, M.P. Johan, T. Furuta, T. Sakaguchi, N. Adachi, Oncolytic effect of a recombinant vesicular stomatitis virus encoding a tumor-suppressor microRNA in an osteosarcoma mouse model, Anticancer Res. 43 (2023) 1185–1191.
[44] Q. Luo, H. Song, X. Deng, J. Li, W. Jian, J. Zhao, et al., A triple-regulated oncolytic adenovirus carrying microRNA-143 exhibits potent antitumor efficacy in colorectal cancer, Mol Ther Oncolytics 16 (2020) 219–229.
[45] N. Sugito, K. Heishima, Y. Akao, Chemically modified MIR143-3p exhibited anti-cancer effects by impairing the KRAS network in colorectal cancer cells, Mol Ther Nucleic Acids 30 (2022) 49–61.
[46] N. Sugito, K. Heishima, Y. Ito, Y. Akao, Synthetic MIR143-3p suppresses cell growth in rhabdomyosarcoma cells by interrupting RAS pathways including PAX3-FOXO1, Cancers (2020) 12.
[47] Y. Ma, C. Li, Y. Huang, Y. Wang, X. Xia, J.C. Zheng, Exosomes released from neural progenitor cells and induced neural progenitor cells regulate neurogenesis through miR-21a, Cell Commun Signal 17 (2019) 019–0418.
[48] W. Ying, M. Riopel, G. Bandyopadhyay, Y. Dong, A. Birmingham, J.B. Seo, et al., Adipose tissue macrophage-derived exosomal miRNAs can modulate in vivo and in vitro insulin sensitivity, Cell 171 (2017) 372–384.
[49] S. Chen, Y. Tang, Y. Liu, P. Zhang, L. Lv, X. Zhang, et al., Exosomes derived from miR-375-overexpressing human adipose mesenchymal stem cells promote bone regeneration, Cell Prolif. 52 (2019) 5.
[50] C. Li, Y. Li, W. Wang, M. Scimeca, G. Melino, R. Du, et al., Deer antlers: the fastest growing tissue with least cancer occurrence, Cell Death Differ. 30 (2023) 2452–2461.
[51] P. Hu, G. Zhang, H. Ba, J. Ren, J. Li, Z. Wang, et al., Reciprocal negative feedback between Prrx1 and miR-140-3p regulates rapid chondrogenesis in the regenerating antler, Cell. Mol. Biol. Lett. 29 (2024) 024–00573.